



COMPARATIVE STUDY OF ACOUSTIC PROPERTIES OF NANOSIZED SUBSTITUTED CALCIUM HEXAFERRITES

S. R. Gawali^{a*}, P. R. Moharkar^b

^aDepartment of Physics, Dr. Ambedkar College, Chandrapur, (M.S.), India (442401)

^bDepartment of Physics, A. C. S. College, Tukum, Chandrapur, (M.S.), India (442401)

*Corresponding author's e-mail: sanjaygawali500@gmail.com

Mobile No.:09422910269

ABSTRACT

The two series of nanosized aluminium and cobalt substituted calcium hexaferrites $\text{Ca}_2\text{Zn}_2\text{Fe}_{12-x}\text{Me}_x\text{O}_{22}$ (Me = Al or Co) have been successfully synthesized by sol-gel auto-combustion route. The structural characteristics of both series of synthesized samples have been studied by X-ray diffraction (XRD) and Scanning electron microscopy (SEM). The acoustic properties of the both series of samples have been investigated by ultrasonic pulse transmission technique. XRD analysis of both series showed that the synthesized samples were single phase Y-type hexagonal ferrites. The SEM study showed that the average particle size of the both series of synthesized samples was found to be in nanorange. The acoustic studies indicate that the increase in elastic moduli with Al^{3+} ions concentration weaken the inter-atomic bonding between various atoms in the substituted calcium hexaferrite where as the decrease in elastic moduli with Co^{3+} ions concentration strengthened the inter-atomic bonding between various atoms in hexaferrite continuously.

Keywords: Y-type hexagonal ferrite, nanoparticles, Sol-gel Auto Combustion route, TEM, acoustic properties etc.

1. Introduction

Hexagonal ferrites have been widely used in the field of material science. The elastic constants of the materials can be determined by studying propagation of ultrasonic waves through those materials. This provides better understanding of the behaviour of the engineering materials. The elastic constants of the material are related with the fundamental solid state phenomenon such as specific heat, Debye temperature and Grunesian parameter. The elastic constants of a material can be determined by measuring the velocity of the longitudinal (v_l) and shear waves (v_s) [1].

The ultrasonic velocities and elastic constants are related to each other [2]. The acoustic Debye temperature of materials used to explain the well known solid state problem like lattice vibrations is determined using ultrasonic velocity.

The elastic constants are related to interatomic forces, co-ordination changes, etc; and also the impact shock, fracture and crack growth [3]. For porous materials like cast metal, ceramics and most composites, the relation between elastic moduli and velocity are complex. The other microstructural factors such as grain shape, grain boundaries, texture and precipitates have pronounced effect on the relation between elastic moduli and velocity [4, 5].

It is essential to understand the relationship between porosity and its elastic behavior in order to improve the mechanical properties of ceramic materials. The measured elastic moduli do not have much significance unless they are corrected to zero porosity.

In the present work, two series of samples of aluminium and cobalt substituted Y-type calcium hexaferrite have been synthesized by sol-gel auto-combustion route. The effect of substitution of Al^{3+} or Co^{3+} ion on structural and acoustic properties calcium hexaferrites have been investigated.

2. Experimental

2.1. Sample preparations

The substituted calcium hexaferrites having the following formula $\text{Ca}_2\text{Zn}_2\text{Fe}_{12-x}\text{Me}_x\text{O}_{22}$ where $\text{Me} = \text{Al}$ or Co with $x = 0$ and 0.5 was synthesized sol-gel auto-combustion route. A stoichiometric amount of AR grade $\text{Ca}(\text{NO}_3)_2 \cdot 4\text{H}_2\text{O}$, $\text{Fe}(\text{NO}_3)_3 \cdot 9\text{H}_2\text{O}$, and $\text{Al}(\text{NO}_3)_3 \cdot 9\text{H}_2\text{O}$ or $\text{Co}(\text{NO}_3)_3 \cdot 9\text{H}_2\text{O}$ were dissolved in a minimum amount of deionized distilled water at the temperature of 50°C under constant stirring. The urea $\text{CO}(\text{NH}_2)_2$ was added to the mixed solution as fuel. The homogeneous aqueous solution was then heated in the digitally controlled microwave oven of 2.45 GHz for 15–20 min so that all water evaporate and leave a viscous dense gel. The final viscous gel burnt by self propagating combustion reaction evolving large volumes of gases (N_2 , NH_3 and H_2NCO) and finally gets converted into a fluffy powder. Ultimately, the resulting powder was calcined at 900°C for 4 hours to form substituted calcium hexaferrite phase [6].

2.2 Characterization

The identification of the crystalline phase was performed using X-ray diffractometer (XRD), model PW 1710 (Philips Holland) with $\text{Cu-K}\alpha$ radiation source, in the range from 20° to 70° with a step of 0.02° for 1 second..

The morphological properties of the synthesized samples are recorded by using SEM studies using Scanning Electron Microscope (Model JSM- 7600F) having resolution of 1.0nm (15kV), 1.5nm (1kV) accelerating voltage 0.1 to 30 kV, magnification X 25 to 1000000.

The acoustic properties of the samples have been investigated by ultrasonic pulse transmission technique [2]. For ultrasonic measurement of both series of samples, they are made in the form of pellets with

diameter 15mm and thickness more than 10mm. The radio frequency pulse generated by a pulse oscillator was applied to quartz transducer and these pulse passes in longitudinally and transverse position of the samples having specified dimensions at 100 KHz. The longitudinal velocity (v_l), transverse velocity (v_s) and mean sound velocity (v_m) were calculated.

The elastic constants of a material can be determined by measuring the velocity of the longitudinal (V_l) and shear wave (V_s) [1]. The ultrasonic velocities and elastic constants are related as given by the following equations.

$$\text{Longitudinal modulus } L = \rho(V_l)^2 \quad \text{.....(1)}$$

$$\text{Rigidity modulus } G = \rho(V_s)^2 \quad \text{.....(2)}$$

$$\text{Bulk modulus } B = L - \frac{4}{3}G \quad \text{.....(3)}$$

$$\text{Poisson's ratio } \sigma = \frac{3B-2G}{6B+2G} \quad \text{.....(4)}$$

$$\text{Young's modulus } E = (1 + \sigma)2G \quad \text{.....(5)}$$

The acoustic Debye temperature of materials used to explain the well known solid state problem like lattice vibrations is determined using ultrasonic velocity. The relation is given as $\theta = \frac{h}{k_B} \left[\frac{3N_A P}{4\pi V} \right]^{\frac{1}{3}} V_m$ (6)

Where h is the Planck's constant, k_B Boltzmann constant, N_A Avogadro number, V volume calculated from the effective molecular weight and the density (i.e. M/ρ), P the number of atoms in the molecular formula

$$\text{and } V_m \text{ the mean sound velocity defined by the relation } v_m = \left[\frac{\frac{2}{v_s^3} + \frac{1}{v_l^3}}{3} \right]^{-\frac{1}{3}} \quad \text{.....(7)}$$

3. Results and discussion

3.1. XRD analysis

XRD patterns of aluminium substituted calcium hexaferrite and cobalt substituted calcium hexaferrite ($x=0, 0.5$ and 1) are shown in Fig. 1. The XRD data analysis was done using computer software PCPDF Win, Powder-X and fullproof software suite. The XRD pattern of both series of samples confirms that the synthesized samples are found to have Y-type hexagonal structure belonging to the space group $R\bar{3}m$ (no. 166).

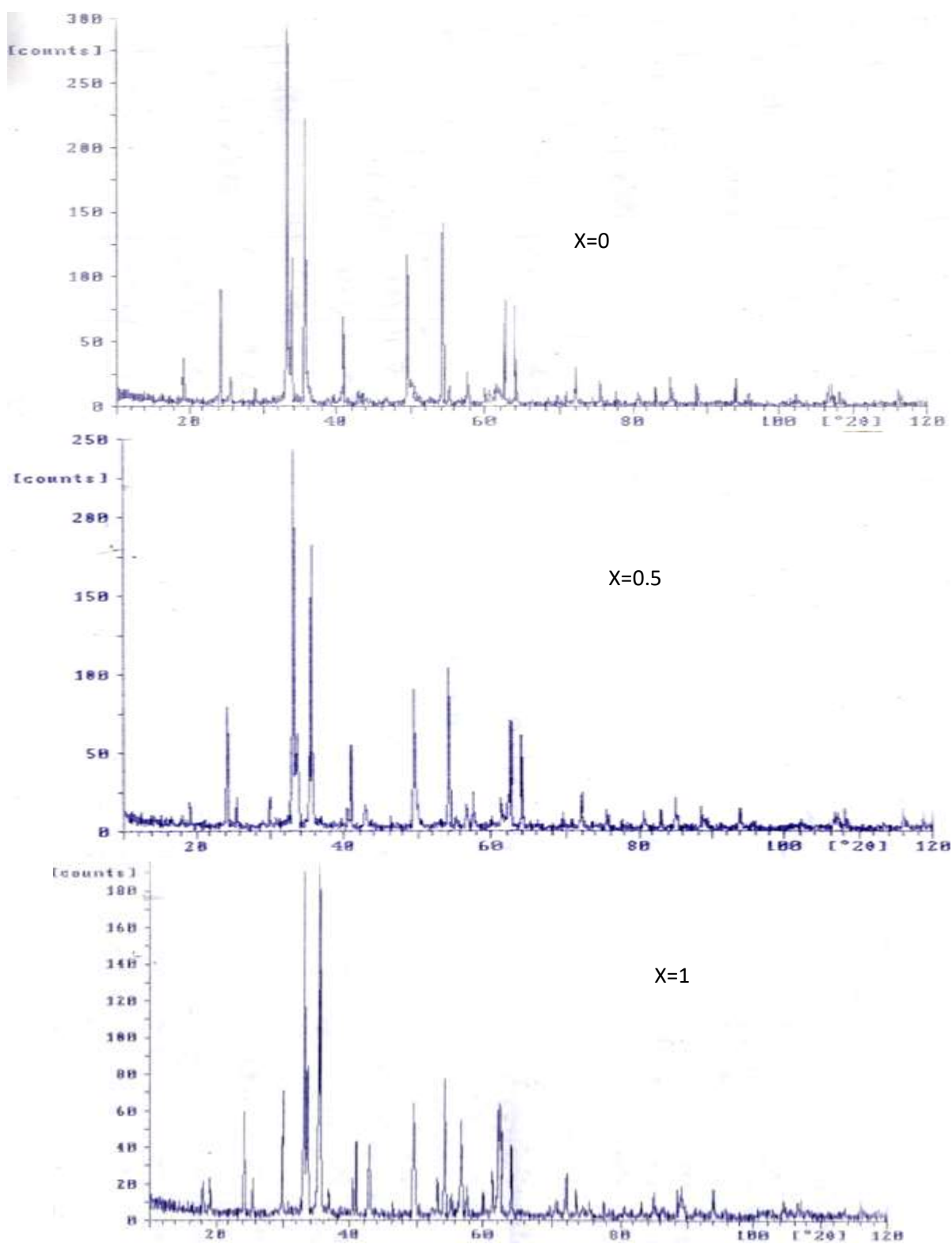


Fig. 1(a): X-ray diffraction spectra of sample $\text{Ca}_2\text{Zn}_2\text{Fe}_{12-x}\text{Al}_x\text{O}_{22}$

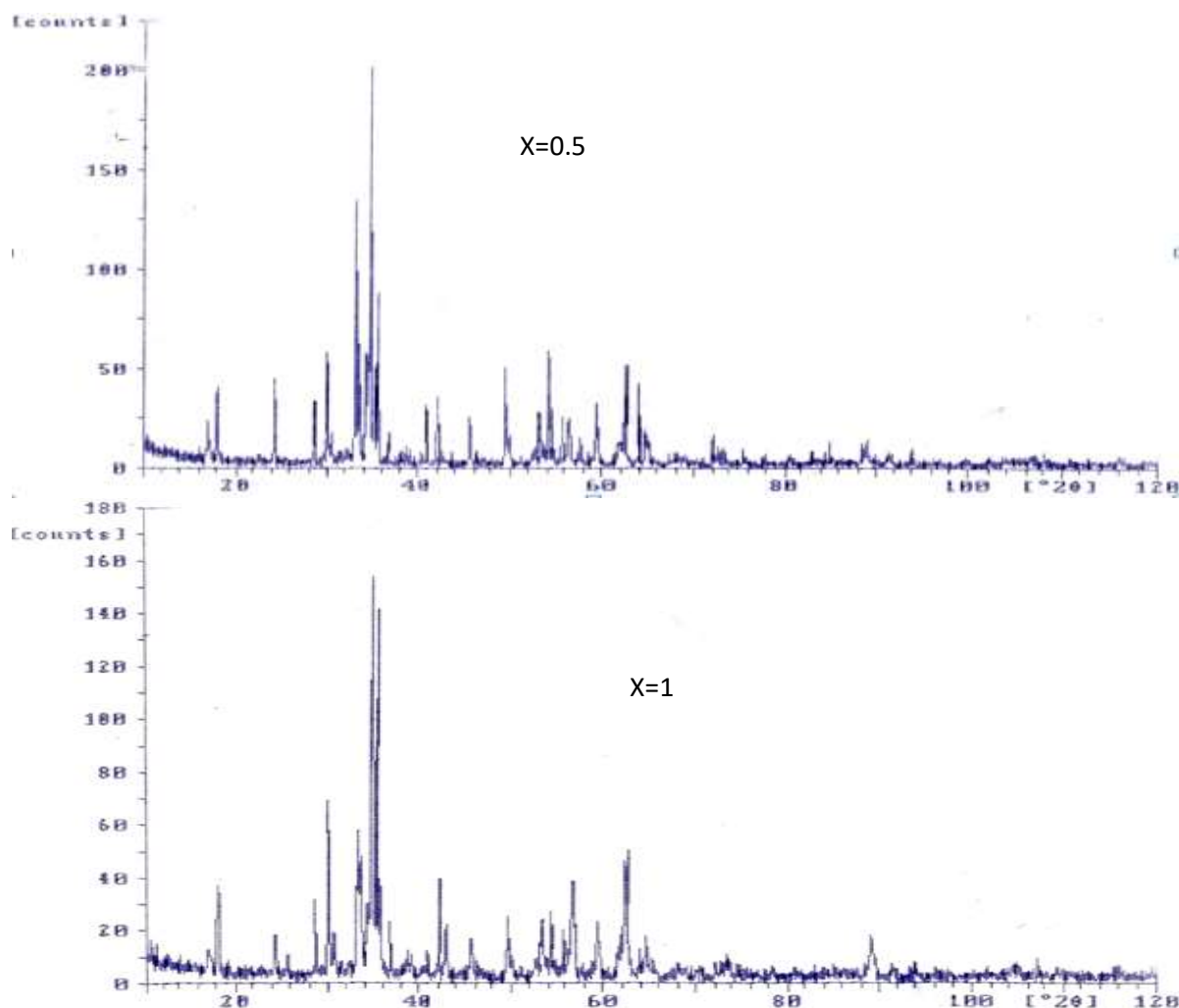


Fig. 1(b). X-ray diffraction spectra of sample $\text{Ca}_2\text{Zn}_2\text{Fe}_{12-x}\text{Al}_x\text{O}_{22}$

The lattice constants a and c , X-ray densities, bulk densities and porosity of the both series of samples at room temperature are given in the Table 1.

Table 1: Lattice constants (a) and (c), cell volume (V), X-ray density ($\rho_{\text{x-ray}}$), bulk density (ρ_{m}) and porosity (P) of samples

Sample	a (Å)	c (Å)	V (Å) ³	$\rho_{\text{x-ray}}$ (gm/cm ³)	ρ_{m} (gm/c m ³)	P (%)
$\text{Ca}_2\text{Zn}_2\text{Fe}_{12}\text{O}_{22}$	5.0390	44.1072	1249.27	4.2239	3.0982	26.67
$\text{Ca}_2\text{Zn}_2\text{Fe}_{11.5}\text{Al}_{0.5}\text{O}_{22}$	5.0452	44.2512	1245.11	4.1507	2.7761	33.11
$\text{Ca}_2\text{Zn}_2\text{Fe}_{11}\text{AlO}_{22}$	5.0446	44.2056	1244.89	4.1067	3.1255	33.90
$\text{Ca}_2\text{Zn}_2\text{Fe}_{11.5}\text{Co}_{0.5}\text{O}_{22}$	5.0418	44.1876	1242.93	4.2168	2.9268	30.60
$\text{Ca}_2\text{Zn}_2\text{Fe}_{11}\text{CoO}_{22}$	5.0274	44.0628	1232.32	4.2583	2.1634	49.20

The cell volume of calcium hexaferrites samples decreases after being doped with Al^{3+} ion and increases after being doped with Co^{3+} ion for Fe^{3+} ion. These results agree well to that reported by Kuhikar and Kulkarni[7], Salunkhe[8] and Moharkar [9].

The lattice parameter ' a ' and ' c ' and ' V ' slightly changes with substitution of Al^{3+} ion in calcium hexaferrite sample. This is due to relatively large ionic radius of Al^{3+} ion (0.53 Å) comparing to that of Fe^{3+} ion (0.64 Å) for six fold coordination. As a result, the cell volume of the samples of hexaferrite decreases after

being doped with Al^{3+} ions. The decrease in X-ray density and bulk densities on substitution of Al^{3+} ion in hexaferrite samples is due to the smaller molar masses of the substituted ion. The X-ray density is higher than the bulk density (ρ_m) which indicates the presence of pores in the synthesized samples. The porosity increases with increase in the Al^{3+} ions content in calcium hexaferrites. These results agree well to that reported by P. R. Moharkar [9], M. B Solunke [10]. It was seen that density and porosity are inversely varies with dopent concentration. This behaviour may be attributed to the fact that introduction of Co^{+3} ions in hexagonal ferrites may affect the grain size development during firing process and decrease the porosity Hemeda and Hemeda [11]. Thus it can be concluded that substitution enhance the firing process and increase the grain size to leading to decrease of porosity.

3.2 SEM analysis

Fig. 2 shows SEM photographs of aluminium substituted calcium hexaferrite and cobalt substituted calcium hexaferrite. From SEM photograph, it can be confirmed that samples exhibit relatively well defined, hexagonal like grains with average size of less than 80nm. The similar results was reported by Thompson [12].

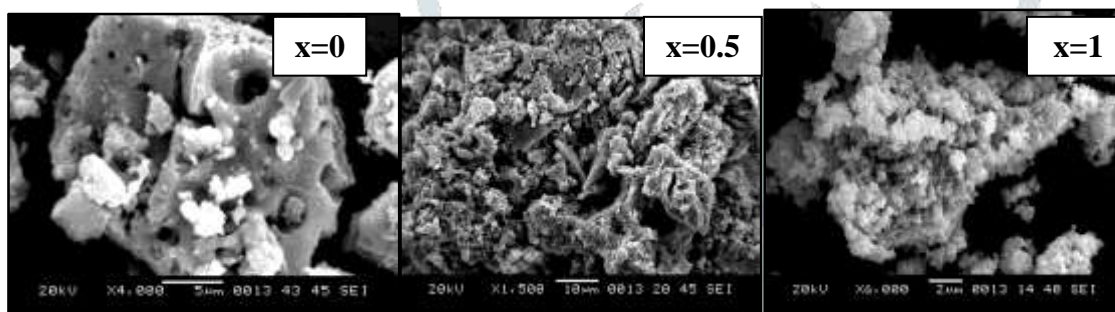


Fig.2 (a): SEM photographs of samples $\text{Ca}_2\text{Zn}_2\text{Fe}_{12-x}\text{Al}_x\text{O}_{22}$

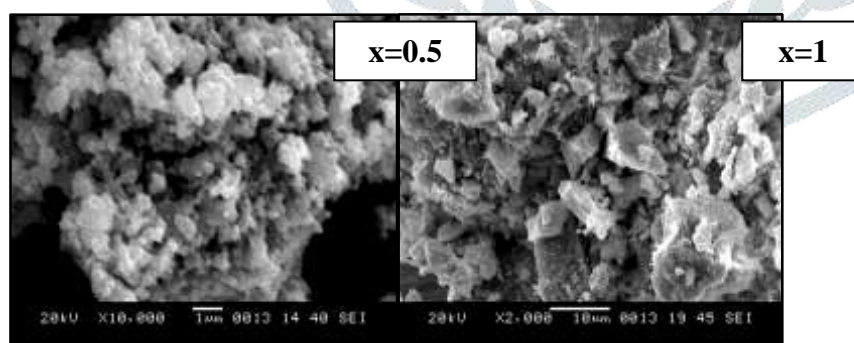


Fig.2 (b): SEM photographs of samples $\text{Ca}_2\text{Zn}_2\text{Fe}_{12-x}\text{Co}_x\text{O}_{22}$

3.3. Acoustic studies

The values of ultrasonic wave velocity and Debye characteristic temperature of the both series of synthesized samples are summarized in Tables 2. Table 3 depicts the values of longitudinal modulus, bulk modulus, Young's modulus, rigidity modulus and Poisson's Ratio with Al content (x).

Table 2: Longitudinal Velocity (V_l), Transverse Velocity (V_s), Mean Sound Velocity (V_m), Mass Density (d), V_l/d ($\text{Kg}^{-1}\text{m}^4\text{s}^{-1}$), V_s/d ($\text{Kg}^{-1}\text{m}^4\text{s}^{-1}$) and Debye Temperature (θ) of the both aluminium and cobalt substituted calcium hexaferrite samples.

Sample	x	V_l (m/s)	V_s (m/s)	V_m (m/s)	$V_l/d(\text{Kg}^{-1}\text{m}^4\text{s}^{-1})$	$V_s/d(\text{Kg}^{-1}\text{m}^4\text{s}^{-1})$	θ (K)
$\text{Ca}_2\text{Zn}_2\text{Fe}_{12}\text{O}_{22}$	0	2333	1700	1600	0.75	0.50	2141.25
$\text{Ca}_2\text{Zn}_2\text{Fe}_{11.5}\text{Al}_{0.5}\text{O}_{22}$	0.5	2636	1503	1833	0.94	0.65	2695.14
$\text{Ca}_2\text{Zn}_2\text{Fe}_{11}\text{AlO}_{22}$	1	2894	2210	1600	0.92	0.65	2703.78
$\text{Ca}_2\text{Zn}_2\text{Fe}_{11.5}\text{Co}_{0.5}\text{O}_{22}$	0.5	2500	1860	1714	0.85	0.58	2222.54
$\text{Ca}_2\text{Zn}_2\text{Fe}_{11}\text{CoO}_{22}$	1	2750	2126	1964	1.27	0.90	1222.63

Table 3: Longitudinal Modulus (L), Bulk Modulus (B), Rigidity Modulus (G), Young's Modulus (E) and Poisson's Ratio (σ) of the both aluminium and cobalt substituted calcium hexaferrite

Sample	X	L (GPa)	B (GPa)	G (GPa)	E (GPa)	σ
$\text{Ca}_2\text{Zn}_2\text{Fe}_{12}\text{O}_{22}$	0	16.86	6.87	7.49	16.47	0.10
$\text{Ca}_2\text{Zn}_2\text{Fe}_{11.5}\text{Al}_{0.5}\text{O}_{22}$	0.5	19.14	6.99	9.11	19.05	0.04
$\text{Ca}_2\text{Zn}_2\text{Fe}_{11}\text{AlO}_{22}$	1	26.17	8.89	12.96	26.16	0.01
$\text{Ca}_2\text{Zn}_2\text{Fe}_{11.5}\text{Co}_{0.5}\text{O}_{22}$	0.5	18.21	6.83	8.59	18.15	0.05
$\text{Ca}_2\text{Zn}_2\text{Fe}_{11}\text{CoO}_{22}$	1	16.36	5.24	8.34	17.01	0.01

It can be seen from the Table 3 that, the longitudinal modulus, bulk modulus, Young's modulus and rigidity modulus increases with increase in Al content (x) following Wooster's work [13], the variation of elastic constant with increase in Al concentration of $\text{Ca}_2\text{Zn}_2\text{Fe}_{12-x}\text{Al}_x\text{O}_{22}$. Superconducting system may be interpreted in term of inter-atomic bonding. Thus, it can be inferred from the increase in elastic moduli with concentration (x) that the inter-atomic bonding between various atoms is being strengthened continuously. The strength of inter-atomic bonding and type of cations are involved in bonding formation. When Fe^{+3} ions is replaced by Al^{+3} ions in $\text{Ca}_2\text{Zn}_2\text{Fe}_{12-x}\text{Al}_x\text{O}_{22}$ system, it improves the elastic behaviour of the system. This finding can be explained on the basis of change in length of inter-atomic bonding. When Fe^{+3} ions with ionic radius (0.64\AA) are replaced by Al^{+3} with smaller ionic radius (0.53\AA), it decrease the bond length and as a result strength of inter-atomic bonding is expected to increase and in turn elastic moduli values. The values of Poisson's ratio varies between 0.01 to 0.10 for all composition, this values in the range from -1 to 0.5 which is in conformity with the theory of isotropic elasticity.

It can be seen from the Table 2 that, the longitudinal modulus, bulk modulus, Young's modulus and rigidity modulus decreases with increase in Co^{+3} ions concentration (x) following Wooster's work [13], the variation of elastic constant decrease with in Co^{+3} ions concentration for Fe^{+3} in $\text{Ca}_2\text{Zn}_2\text{Fe}_{12-x}\text{Co}_x\text{O}_{22}$.

Superconducting system may be interpreted in term of inter-atomic bonding. When Fe^{+3} ion is replaced by Co^{+3} ions in $\text{Ca}_2\text{Zn}_2\text{Fe}_{12-x}\text{Co}_x\text{O}_{22}$ system, it improves the elastic behaviour of the system. This finding can be explained on the basis of change in length of inter-atomic bonding. When Fe^{+3} ions with ionic radius (0.64\AA) are replaced by Co^{+3} ion with larger ionic radius (0.68\AA), it increase the bond length and as a result strength of inter-atomic bonding is expected to decrease and in turn elastic moduli values.

The observed increase in Debye temperature (θ) (Table 2) with Al^{3+} ions concentration suggested that the lattice vibrations are decrease due to aluminium ions substitutions where as the observed decrease in Debye temperature (θ) (Table 2) with Co^{3+} ions concentration suggested that the lattice vibrations are increase due to cobalt ions substitutions.. The magnitude of elastic constants and Debye temperature are constant with other Bi2212 based superconducting systems.

4. Conclusion

The aluminium and cobalt substituted calcium ferrites were synthesized by sol-gel auto-combustion route. The X-ray diffraction studies of both series confirm the formation of monophasic Y-type hexagonal ferrites and the values of a and c of the sample supports this confirmation. The space group for the both series of samples was observed to be $R\bar{3}m$ (SG no. 166).

The SEM study of the both series of sample showed that the average particle size is found to be in nano-range. The acoustic studies indicate that the increase in elastic moduli with Al^{3+} ions concentration weaken the inter-atomic bonding between various atoms in the substituted calcium hexaferrite where as the decrease in elastic moduli with Co^{3+} ions concentration strengthened the inter-atomic bonding between various atoms in hexaferrite continuously.

References

- [1] Schrieber E., Anderson O., Soga N., Elastic Constant and their Measurement, *McGraw Hill Publishing Ltd.*, New York, (1973).
- [2] Baldev Raj V., Rajendran P., *Palanichamy Science & Technology of ultrasonics*, Narosa Publishing House, New Delhi, p. 250 (2004).
- [3] Kannine M., Oioekar C., *Advanced Fracture Mechanics*, Oxford Clarendon Press, 392 (1985).
- [4] Serabian S., *British J NDT* 22, 69 (1980).
- [5] Green R., in Buck O., Wolf S. (Eds.), *NDE Microstructure Characterisation and Reliability Strategies*, *Warrendale MSAIME*, P. 199, (1981).
- [6] Lengule S. B., Moharkar P. R., Gawali S. R. and Rewatkar K. G., *Int. Journal of Res. in Bio. Agri. And Tech.*, Vol. II, Issue (7), Nov 2015: 178-181.
- [7] S. Kuhikar, D. Kulkarni, *Inter.J. Phys. Sci.* Vol.17 (2) (2005) 333-338.
- [8] M. Solunke, N. Lanje, D. Kulkarni, *Ind. J. Pure App. Phys.* 40(2002) 301-303.
- [9] Moharkar P.R., Gawali S.R., Rewatkar K.G., Sable S.N., and Nanoti V.M., (2012), *Inter. J. Know. Engi.* 3 (1) 113-115

- [10] Solunke M.B., Sharma P.U., Lakhani V.K., Pandya M.P., Modi K.B., Reddy P.V., Shah S.S. (2007) Ceram. Inter. 33, 21-26.
- [11] Hemeda D.M. and Hemeda O.M., American Journal of Applied Science **5**(4): 289- 295(2008).
- [12] Thompson, Simon; Shirtcliffe, Neil J.; O'Keefe, Eoin S.; Appleton, Steve; Perry, Carole C., Journal of Magnetism and Magnetic Materials **292**, 100-107(2005).
- [13] Wooster W.A., *Rep Pro. Phys.*, **16**, 62 (1953).

